

Rapid Commun. Mass Spectrom. 2016, 30, 2529–2536
(wileyonlinelibrary.com) DOI: 10.1002/rcm.7742

Characterization of post-translational modifications on lysine 9 of histone H3 variants in mouse testis using matrix-assisted laser desorption/ionization in-source decay

Ho-Geun Kwak^{1,2} and Naoshi Dohmae^{1,2*}

¹Biomolecular Characterization Unit, RIKEN Center for Sustainable Resource Science, 2-1 Hirosawa, Wako 351-0198, Japan

²Graduate School of Science and Engineering, Saitama University, Saitama, Saitama 338-8570, Japan

RATIONALE: Post-translational modifications (PTMs) of histones result in changes to transcriptional activities and chromatin remodeling. Lysine 9 of histone H3 (H3K9) is subject to PTMs, such as methylation and acetylation, which influence histone activity during spermatogenesis. Characterization strategies for studying PTMs on H3K9 have been developed to provide epigenetic and proteomic information. Proteomic analysis has been used to limited success to study PTMs on H3K9; however, a comprehensive analytical approach is required to elucidate global patterns of PTMs of H3 variants during spermatogenesis. **METHODS:** Intact H3 variants in mouse testis were separated by high-performance liquid chromatography on a reversed-phase column with an ion-pairing reagent. Modifications to H3K9 were identified *via* top-down analysis using matrix-assisted laser desorption/ionization in source decay (MALDI-ISD).

RESULTS: Mono-, di-, and tri-methylations were identified at H3K9 in mouse testis and epididymis. These modifications were also observed in testis-specific histone H3 (H3t). Specifically, tri-methylation was more abundant on H3tK9 than on K9 of other H3 variants.

CONCLUSIONS: We introduce a method for rapid, simple, and comprehensive characterization of PTMs on the N-termini of H3 variants using MALDI-ISD. This approach provides novel and useful information, including K9 modifications on H3t, which would benefit epigenetic and proteomic research. © 2016 The Authors. *Rapid Communications in Mass Spectrometry* Published by John Wiley & Sons Ltd.

Multiple post-translational modifications (PTMs) decorate the N-termini of histone H3 variants, including methylation and acetylation.^[1–3] The modification of H3 variants plays a key role in regulation of chromatin structure, which is correlated with the active (euchromatin) and repressed (heterochromatin) states; current research on the biological activities of H3 variants has focused on understanding these functional and structural features.^[4,5] Methylation and acetylation of lysines K4, K9, K18, K23, and K27 are commonly observed on the N-tails of H3 variants.^[4,5] Of these, K9 is particularly well studied as a site for methylation and acetylation.^[4,5] K9 modification of H3 variants (H3K9) has been reported as being related to transcriptional regulation and chromatin dynamics.^[4–7] The expression of testis-specific histone H3 (H3t) and the methylation and acetylation of H3K9 are both detected during spermatogenesis.^[6,7] H3t is primarily expressed during spermatogenesis (detected only

at low levels in somatic tissues), and is thought to be associated with chromatin remodeling; however, additional research is needed to confirm its activities and PTMs.^[7]

To understand the structural and functional features of specific modification patterns on H3K9 during spermatogenesis, experimental approaches have been developed.^[6–9] During spermatogenesis, H3K9 modifications have been detected by proteomic approaches such as mass spectrometry (MS) and antibody-based methods.^[8–12] Acetylated and methylated H3K9s during spermatogenesis have been identified by immunostaining analysis.^[10–12] However, these traditional approaches do not include information about which H3 variant is being detected, nor a comprehensive analysis of co-occurring PTMs.^[10–12] MS-based identification has become the preferred approach to characterize the PTMs on histones, as it offers improved sensitivity, simplicity, and compatibility with separation steps, as compared to antibody-based strategies.^[1,3] Garcia *et al.* characterized mono-, di-, and tri-methylations on H3.2 and H3.3 in rat testis using the middle-down strategy with MS.^[8] In addition, a bottom-up approach using nanospray liquid chromatography/tandem mass spectrometry (nano-LC/MS/MS) enables the identification of various PTMs on H3 variants during spermatogenesis, including acetylation and methylation.^[9] Although these MS-based studies enable characterization of PTMs on H3 variants, the identification of PTMs on specific sequences of H3 variants, including H3t, remains a challenge.

* Correspondence to: N. Dohmae, Biomolecular Characterization Unit, RIKEN Center for Sustainable Resource Science, 2-1 Hirosawa, Wako 351-0198, Japan.
E-mail: dohmae@riken.jp

This is an open access article under the terms of the Creative Commons Attribution-NonCommercial License, which permits use, distribution and reproduction in any medium, provided the original work is properly cited and is not used for commercial purposes.

MS-based top-down approaches have been developed to resolve the demerits of digestion-based methods. The main advantage of this strategy is that intact protein step-analysis protects against the loss of modifications, allowing characterization of PTMs without a digestion step being performed.^[1–3] The top-down analysis using matrix-assisted laser desorption/ionization in source decay (MALDI-ISD) is a practical and effective tool for characterizing intact proteins and their PTMs, specifically at their N- or C-termini. This method is capable of simple and quick analysis with useful cleavages (c-, y-, and (z+2)-ions), allowing characterization of protein sequences without losing PTMs on histone tails.^[13] MALDI-ISD has been successful in characterization of multiple proteins and their modifications,^[13–15] however, it has not yet been applied to study histones and their PTMs.

Here, we report MALDI-ISD analysis for the characterization of PTMs on histone H3 variants isolated from mouse testis and epididymis. The N- and C-termini of H3 variants were successfully characterized by the fragmentation with c-, y-, and (z+2)-ions. Mono-, di-, and trimethylations were detected at K9 in mouse testis and epididymis. These modifications were also observed in H3t. We observed a greater abundance of trimethylation on H3tK9 than on the K9 of other H3 variants.

EXPERIMENTAL

Reagents

Trichloroacetic acid (TCA), hydrochloric acid (HCl), potassium chloride (KCl) magnesium acetate ($\text{Mg}(\text{CH}_3\text{COO})_2$) and dithiothreitol (DTT) were purchased from Wako Pure Chemicals (Osaka, Japan). Trizma base was from Sigma-Aldrich (St. Louis, MO, USA) and sulfuric acid (H_2SO_4) was obtained from Junsei Chemical Co. (Tokyo, Japan). Trifluoroacetic acid (TFA, Merck, Darmstadt, Germany), heptafluorobutyric acid (HFBA, Thermo-Fisher Scientific, Waltham, MA, USA), and acetonitrile (Thermo-Fisher Scientific, Waltham, MA, USA) were HPLC grade.

Extraction of histones from mouse testes

Mouse (BALB/c) testes combined with epididymides were purchased from Funakoshi Co. (Tokyo, Japan) and homogenized following separation. Whole histones were extracted from testis and epididymis using the TCA-

precipitation method with minor modifications.^[16] In brief, all steps were carried out at 4°C. Testis (136.3 mg) and epididymis (392.1 mg) tissues were suspended in hypertonic lysis buffer (10 mM Tris-Cl (pH 8.0), containing 1 mM KCl, 1.5 mM $\text{Mg}(\text{CH}_3\text{COO})_2$, 1 mM DTT, and protease inhibitors) and incubated for 30 min. Lysed cells were pelleted by centrifugation at 10,000 g for 10 min, resuspended in 0.4 N H_2SO_4 , and incubated for 30 min. To collect the histones from the supernatant, nuclear debris was pelleted by centrifugation at 16,000 g for 10 min, and the supernatant was precipitated by adding TCA to a final concentration of 33% and incubated for 30 min. The precipitates were pelleted by centrifugation at 16,000 g for 10 min. After washing with acetone and drying at room temperature, samples were dissolved in 100 μL MilliQ water.

Separation of histone variants

H3 variants, including H3t, were separated using an Agilent high-performance LC 1100 series (Agilent Technologies, Santa Clara, CA, USA) using a C4 RP column (2.0 mm \times 15.0 mm, 3 μm particle size; GL sciences, Tokyo, Japan) at room temperature. A 20- μL sample was injected and detected at a UV wavelength of 215 nm. HFBA was used as an ion-pairing reagent. The mobile phases A (5% acetonitrile with 0.1% HFBA) and B (90% acetonitrile with 0.1% HFBA) were delivered at a flow rate of 0.1 mL/min using the following gradient parameters: 0 to 5 min, 15% solvent B; 5 to 15 min, 15–48% solvent B; 15 to 25 min, 48% solvent B; 25 to 100 min, 48–62% solvent B; 100 to 120 min, 62–100% solvent B; 120 to 130 min, 100% solvent B; 130 to 135 min, 100–15% solvent B; 135 to 145 min, 15% solvent B. The fraction collector (Gilson, Middleton, WI, USA) was programmed to collect fractions at 30 s intervals from 60 to 105 min.

Matrix and analyte preparation

Super DHB (sDHB; 90:10 mixture of 2,5-dihydroxybenzoic acid and 2-hydroxy-5-methoxybenzoic acid) and 1,5-diaminonaphthalene (DAN) were used as the matrix. A saturated solution was prepared in 50% acetonitrile/50% water containing 0.1% TFA. Separated histone H3 variants were dried, and mixed with 10 μL of 30% acetonitrile/70% water containing 0.1% TFA. A 1 μL volume of each sample was air-dried at room temperature on the MALDI plate (MTP 384 polished steel) and mixed with the 1 μL of each sDHB and 1,5-DAN mixtures as analytes.

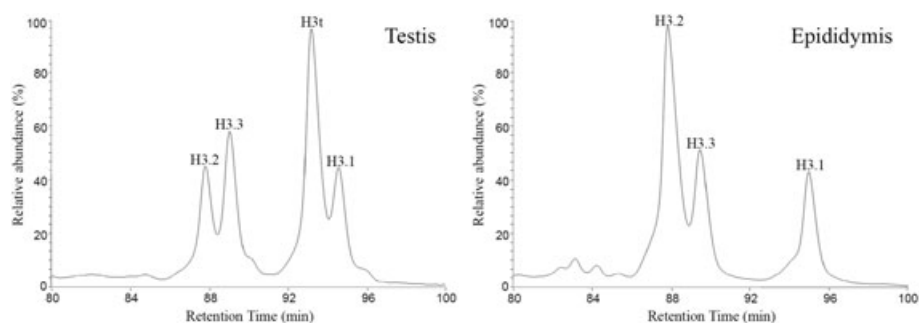


Figure 1. Separation of H3 variants from mouse testis and epididymis. Histone H3 variants from mouse testis (left) and epididymis (right) were separated by HPLC on a C4 RP column with HFBA.

Table 1. Quantification of H3 variants based on areas of peaks

Histone	Areas (Average \pm SD, %)	
	Testis	Epididymis
H3.2	17.3 \pm 0.1	54.6 \pm 0.5
H3.3	23.5 \pm 0.2	24.5 \pm 0.2
H3t	41.5 \pm 0.03	ND
H3.1	17.7 \pm 0.3	20.9 \pm 0.2

Areas of H3 variants were calculated from the integrated peaks on chromatograms, and expressed as percentages relative to the total peak area. The data are shown as averages \pm SD ($n = 3$). The increase in H3.2 in the epididymis as approximately roughly correlated with the loss of H3t in the testis. ND, Not detected.

Identification of histone H3 variants and their PTMs

All processes for the characterization of histone H3 variants and their PTMs were performed by UltrafleXtreme MALDI-TOF (time of flight)-TOF/MS (Bruker Daltonics, Billerica, MA, USA) equipped with a Smartbeam II laser (2 kHz laser repetition rate and 44 μ J/pulse laser). ISD analysis was conducted in reflectron mode within the range of 400–8000 m/z with a 25.00 kV acceleration voltage. The lens voltage was set to 8.00 kV and 26.45 kV was used as the

reflector voltage. The pulsed ion extraction delay and matrix suppression cut-off mass were set to 200 ns and 400 m/z , respectively. The calibration of ISD spectra was externally conducted using c-ion fragments (within the range of 1000–4000 m/z) that were generated from bovine serum albumin.

Data analysis

Each histone H3 variant fraction was identified by peptide-mass fingerprinting (PMF) in advance (data not shown). Fragment ions and K9 modifications (mono-, di-, and trimethylation) were calculated using the GPMW 6.1 software (Lighthouse Data, Odense, Denmark), and ISD spectra of H3 variants were characterized by flexAnalysis (version 3.4, Bruker Daltonics). The sequences of histone H3 variants were obtained from a database (NCBIInr) and previous work on H3t.^[17] Each ion from ISD spectra was corresponded with the calculated data by the GPMW 6.1 software within 50 ppm.

RESULTS AND DISCUSSION

Separation of H3 variants

H3 variants were successfully separated from the testis and epididymis by HPLC using a C4 RP column with HFBA (Fig. 1). Each histone H3 variant peak was identified by PMF in advance (data not shown). An abundance of H3t was

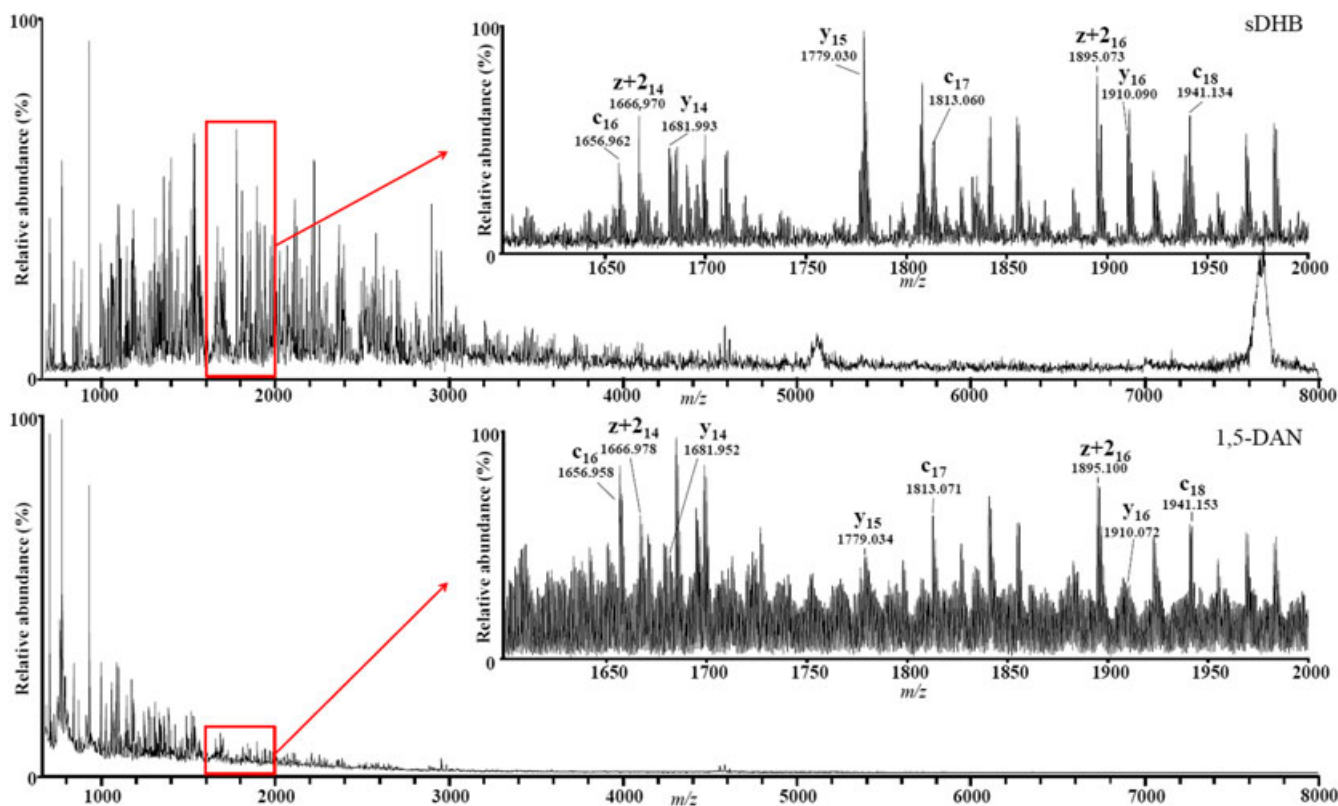


Figure 2. sDHB provides increased sensitivity over 1,5-DAN in MALDI-ISD analysis of H3 variants. ISD spectra at the range of m/z 1600–2000 were magnified to detect fragment ions in detail. c-, y-, and (z+2)-ions were calculated using the GPMW 6.1 software (Lighthouse data, Odense, Denmark). ISD spectra of H3 variants were characterized with flexAnalysis (version 3.4, Bruker Daltonics).

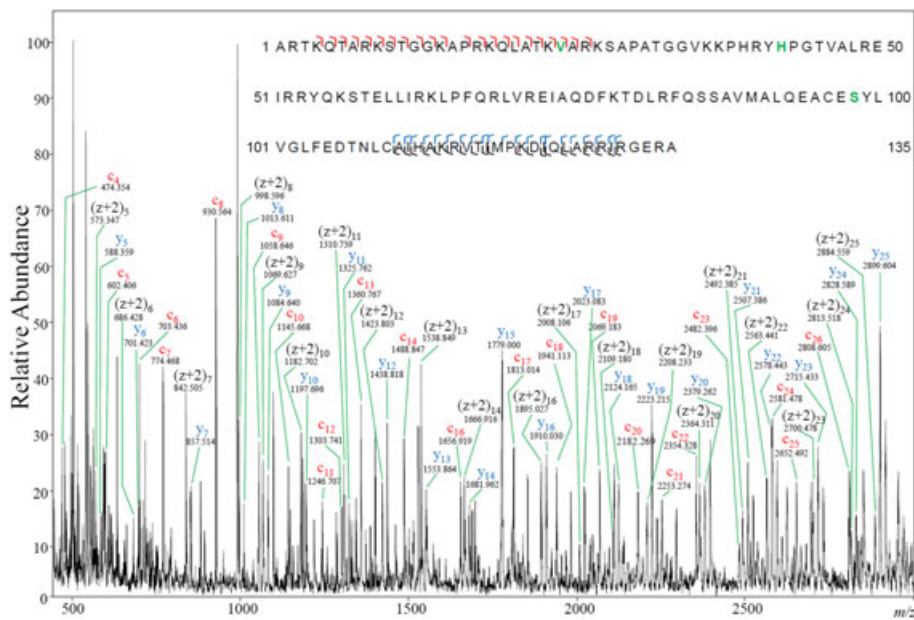


Figure 3. Sequencing H3t tails by fragment ions in the ISD spectrum. Red, c-ions; Blue, y-ions; Black, (z+2)-ions. Fragmentation ions were generated by MALDI-ISD. c-, y-, and (z+2)-ions were calculated using the GPMW 6.1 software (Lighthouse data, Odense, Denmark). ISD spectra of the H3 variants were characterized by the flexAnalysis (version 3.4, Bruker Daltonics). The sequences of histone variants were searched against the database (NCBIInr) and another study.^[17]

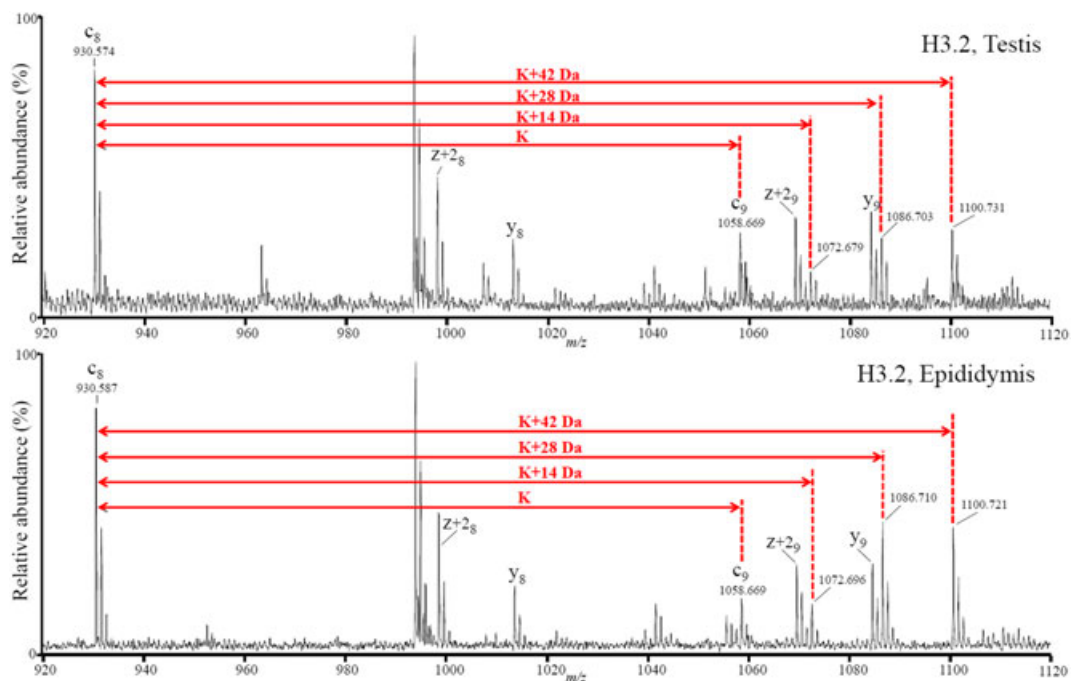


Figure 4. Identification of K9 modifications on H3.2 in mouse testis and epididymis. +14 Da for monomethylation, +28 Da for dimethylation, and +42 Da for trimethylation were set as K9 modifications. Fragment ions were generated by MALDI-ISD. c-, y-, and (z+2)-ions were calculated using the GPMW 6.1 software (Lighthouse data, Odense, Denmark). ISD spectra of H3 variants were characterized by the flexAnalysis (version 3.4, Bruker Daltonics).

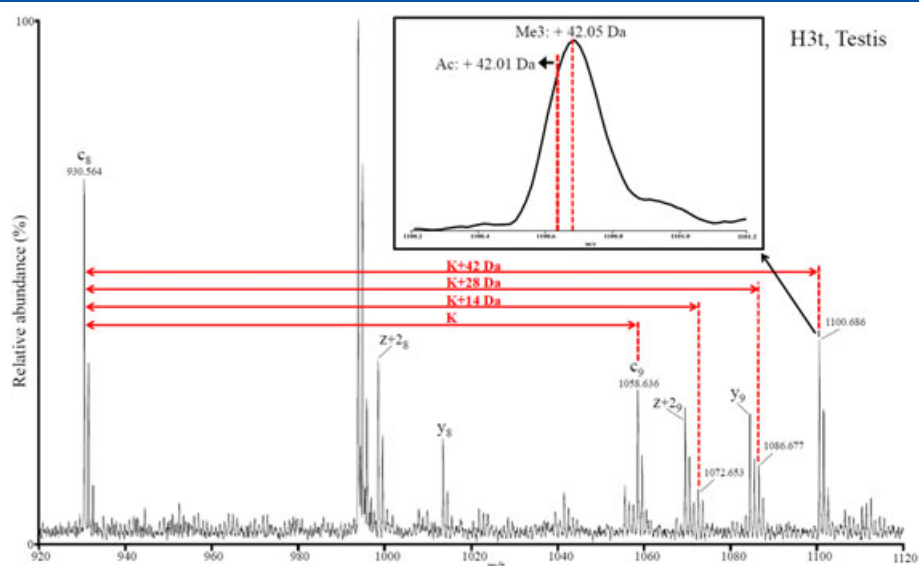


Figure 5. Modifications to K9 of testis-specific histone H3. The shifts of K9 trimethylation of H3t were calculated as 42.046 ± 0.006 Da (mean \pm SD; $n = 3$). Fragment ions were generated by MALDI-MS/MS. *c*-, *y*-, and (*z*+2)-ions were calculated using the GPMW 6.1 software (Lighthouse data, Odense, Denmark). MS/MS spectra of H3 variants were characterized by the flexAnalysis (version 3.4, Bruker Daltonics).

observed in mouse testis, whereas it was undetectable in the epididymis (Fig. 1). A higher abundance of H3.2 was observed in the epididymis, compensating for approximately 90% of the loss of H3t (Table 1). H3t is known to be highly expressed during spermatogenesis, with only a small amount detectable in somatic cells.^[6,7] Consistent with this fact, we detected H3t expression in mouse testis, but its concentration was dramatically reduced in the epididymis.

Choice of matrix for MALDI-MS/MS analysis

The choice of matrix plays an important role in MALDI-TOF analysis. Specifically, an adequate matrix must be chosen to enhance the analytical quality in the ionization.^[13,18] sDHB and 1,5-DAN have become the universal and representative matrices for fragmentation in MALDI-MS/MS analysis.^[15,18,19] We compared these two matrices to investigate their fragmentation efficiency for MALDI-MS/MS analysis of H3 variants (Fig. 2). Overall, sDHB showed a higher sensitivity than 1,5-DAN, particularly within the range of *m/z* 2000–3000 from the N- or C-termini-containing amino acids such as lysine and arginine (Fig. 2). The use of 1,5-DAN enhanced the specific intensities of *c*- and (*z*+2)-ions in MALDI-MS/MS analysis.^[15,19] We observed a higher sensitivity for *c*- and (*z*+2)-ions than *y*-ions when using 1,5-DAN; however, *y*-ions were of limited effectiveness for characterizing C-termini because of their low intensities relative to *y*-ion intensity generated using sDHB (Fig. 2). Our results demonstrated that sDHB can be efficiently used as a matrix for the characterization of histone tails.

Sequencing H3 variant tails

We identified the sequences of histone H3 tails using MALDI-MS/MS. MS/MS fragments, including *c*-, *y*-, and (*z*+2)-ions, were calculated using the GPMW 6.1 software, and these values were correlated with ions in the spectra. MALDI-MS/MS is a

powerful tool for characterizing the termini of intact proteins by fragmentation to generate *c*-ions from N-tails and *y*- and (*z*+2)-ions from C-tails.^[13,15] We detected a total of 63 *c*-, *y*-, and (*z*+2)-ions in the mass spectrum of H3t (*m/z* 450–3000; Fig. 3). Although other histone H3 variants (H3.1, H3.2 and H3.3) have identical sequences at the N- and C-termini, the testis-specific histone H3 contains one amino acid substitution, valine24 (V24), at its N-tail.^[17] We also observed one different amino acid (*c*24-ion, V) at the N-terminus of H3t (Fig. 3). Although MALDI-MS/MS is limited to analyzing whole proteins, we demonstrate here that H3t can be identified and characterized based on the sequence of the N- and C-termini alone.

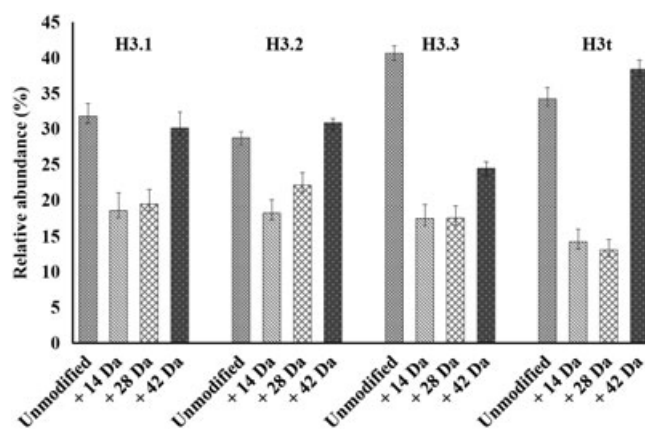


Figure 6. K9 modifications on the N-termini of H3 variants from mouse testis. Relative abundances were calculated from the intensities of monoisotopic molecular ions. Overlapping portions of monoisotopic molecular ions (+14 Da and +28 Da) were subtracted from the isotopic ions of fragment ion (ARRIRGERA), which was indicated in (*z*+2)₉ and *c*₉. Fragment ions were calculated using the GPMW 6.1 software (Lighthouse data, Odense, Denmark).

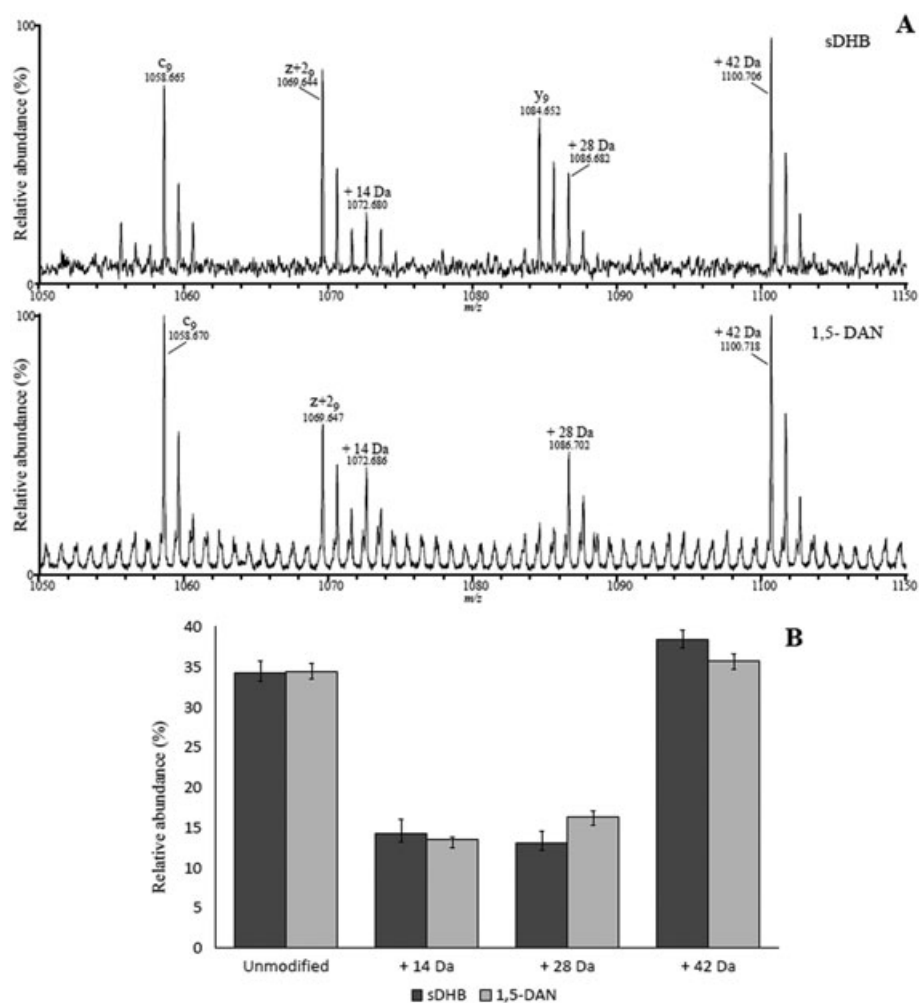


Figure 7. Comparison between sDHB and 1,5-DAN for the characterization of K9 modifications. (A) ISD spectra of H3t K9 modifications using sDHB (top) and 1,5-DAN (bottom). Fragment ions were generated by MALDI-ISD. c -, y -, and $(z+2)$ -ions were calculated using the GPMW 6.1 software (Lighthouse data, Odense, Denmark). ISD spectra of H3t were characterized by the flexAnalysis (version 3.4, Bruker Daltonics). (B) Relative abundances of H3t K9 modifications were calculated from the intensities of monoisotopic molecular ions. Overlapping portions of monoisotopic molecular ions (+14 Da and +28 Da) were subtracted from the isotopic ions of the fragment ion (ARRIRGERA), which was indicated in $(z+2)_0$ and c_0 .

Characterization of K9 methylations of H3t in mouse testis

The mass spectra of the monoisotopic masses of K9 in H3 variants revealed H3K9 modifications, with shifts of +14 Da (monomethylation), +28 Da (dimethylation), and +42 Da (trimethylation) detected (Fig. 4 and Supporting Information). Trimethylation (about 42.047 Da) has a similar, but slightly different, monoisotopic mass as acetylation (about 42.011 Da).^[3] We scored a modification as trimethylation based on the shift of monoisotopic masses (Fig. 5). For example, the shifts of K9 trimethylation of H3t were calculated as 42.046 ± 0.006 Da (mean \pm SD; $n = 3$; Fig. 5). PTMs on H3K9 during spermatogenesis are typically identified by immunostaining.^[10–12] Antibody-based techniques display excellent sensitivity for detecting histone PTMs; however, technical challenges remain, such as time for sample preparation, cross-reactivity of antibodies, and non-compatibility with other analytical instruments, which

limit the comprehensive characterization.^[1,3,20] MS has become the common tool for characterizing PTMs on histones, with accuracy, speed, convenience as its strengths.^[1–3,20] In particular, MALDI-ISD MS, which specifically measures protein tails, is a fast and robust tool to characterize their PTMs in a top-down approach.^[13] In this study, our MS-based approach using MALDI-ISD demonstrated a comprehensive screening of K9 modifications on the N-termini of H3 variants, including H3.1, H3.2, H3.3, and H3t, in mouse testis and epididymis (Figs. 4–6). We observed a greater intensity of K9me2 in the epididymis than in the testis (Fig. 4). Garcia *et al.* detected K9me1, me2, and me3 in H3 variants without H3.1 and H3t from rat testis using a middle-down analysis with ECD fragmentation.^[8] The relative abundances observed increased in the order of K9me3 > unmodified K9 > K9me2 > K9me1 on H3.2, and unmodified

K9 > K9me3 > K9me2 > K9me1 on H3.3.^[8] We observed similar patterns of K9 modification of H3.2 and H3.3 (Fig. 6). Using our approach, we successfully characterized K9 modifications on H3.1 and H3t in mouse testis (Figs. 5 and 6), which had not previously been detected using MS-based approaches. Recent research has also reported the identification of H3K9 me1, me2, and me3 during mouse spermatogenesis using a bottom-up strategy with nano-LC/MS/MS; however, the identification of specific H3 variants was not indicated.^[9]

The testis-specific histone H3, H3t, is highly expressed during spermatogenesis.^[6,7] Although the specific functional role of H3t is still unknown, characterization has been underway, using various proteomic strategies to map its sequence.^[8,17] Despite these advances, the characterization of PTMs on H3t have lagged. In this study, we identified mono-, di-, and trimethylation based on three mass differences (Fig. 5). In particular, trimethylation was more abundant on K9 of H3t in mouse testis than on the K9 of other H3 variants (Figs. 5 and 6). Our findings revealed specific PTMs on K9 of H3t in mouse testis, which will contribute to further research on the functional roles of H3t.

Application of 1,5-DAN to characterize K9 dimethylation

From the mass spectrum of H3t analyzed by sDHB, we detected monoisotopic ions of methylation (+14 Da) and dimethylation (+28 Da), which overlapped with (z+2)₉ and y₉ fragments, respectfully (Fig. 7(A)). The monoisotopic ion of y₉ more closely overlapped with the monoisotopic mass of H3K9me2 (Fig. 7(A)). 1,5-DAN, the matrix for ISD analysis, is specific for generating c- and (z+2)-ions.^[15,19] We found the use of 1,5-DAN generated a weaker abundance of y-ions, compared to c- and (z+2)-ions (Fig. 3). To investigate the consistency of results across both matrices, we characterized K9 dimethylation using 1,5-DAN. We observed a decreased abundance of y₉-ions with 1,5-DAN, compared to the spectrum from sDHB (Fig. 7(A)). Despite this difference, we observed similar patterns of K9 methylation using either matrix (Fig. 7(B)).

CONCLUSIONS

In this study, H3 variant tails and their PTMs were identified in mouse testis and epididymis by top-down characterization using MALDI-ISD. We successfully detected mono-, di-, and trimethylations of H3K9 in mouse testis and epididymis. Specifically, a higher abundance of trimethylation of K9 was observed on H3t compared to other H3 variants. MALDI-ISD analysis allows for the simple, rapid, and comprehensive analysis of PTMs on the N- or C-termini of histones. This approach provides novel and useful information, including K9 modifications on H3t, which provide a basis for further epigenetic and proteomic research.

Acknowledgement

A portion of this research was supported by the RIKEN International Program Associate.

REFERENCES

- [1] B. A. Garcia, J. Shabanowitz, D. F. Hunt. Characterization of histones and their post-translational modifications by mass spectrometry. *Curr. Opin. Chem. Biol.* **2007**, *11*, 66.
- [2] A. M. Arnaudo, B. A. Garcia. Proteomic characterization of novel histone post-translational modifications. *Epigenetics Chromatin* **2013**, *6*, 24.
- [3] A. Moradian, A. Kalli, M. J. Sweredoski, S. Hess. The top-down, middle-down, and bottom-up mass spectrometry approaches for characterization of histone variants and their post-translational modifications. *Proteomics* **2014**, *14*, 489.
- [4] Y.M. Xu, J.Y. Du, A. T. Lau. Posttranslational modifications of human histone H3:an update. *Proteomics* **2014**, *14*, 2047.
- [5] C. E. Thomas, N. L. Kelleher, C. A. Mizzen. Mass spectrometric characterization of human histone H3: a bird's eye view. *J. Proteome Res.* **2006**, *5*, 240.
- [6] C. Rathke, W. M. Baarends, S. Awe, R. Renkawitz-Pohl. Chromatin dynamics during spermiogenesis. *Biochim. Biophys. Acta* **2014**, *1839*, 155.
- [7] J. Bao, M. T. Bedford. Epigenetic regulation of the histone-to-protamine transition during spermatogenesis. *Reproduction* **2016**, *151*, R55.
- [8] B. A. Garcia, C. E. Thomas, N. L. Kelleher, C. A. Mizzen. Tissue-specific expression and post-translational modification of histone H3 variants. *J. Proteome Res.* **2008**, *7*, 4225.
- [9] L. J. Luense, X. Wang, S. B. Schon, A. H. Weller, E. Lin Shiao, J. M. Bryant, M. S. Bartolomei, C. Coutifaris, B. A. Garcia, S. L. Berge. Comprehensive analysis of histone post-translational modifications in mouse and human male germ cells. *Epigenetics Chromatin* **2016**, *9*, 24.
- [10] C. Rathke, W. M. Baarends, S. Jayaramaiah-Raja, M. Bartkuhn, R. Renkawitz, R. Renkawitz-Pohl. Transition from a nucleosome-based to a protamine-based chromatin configuration during spermatogenesis in *Drosophila*. *J. Cell Sci.* **2007**, *1*, 1689.
- [11] N. Song, J. Liu, S. An, T. Nishino, Y. Hishikawa, T. Koji. Immunohistochemical analysis of histone H3 modifications in germ cells during mouse spermatogenesis. *Acta Histochem. Cytochem.* **2011**, *44*, 183.
- [12] C. Steilmann, A. Paradowska, M. Bartkuhn, M. Vieweg, H. C. Schuppe, M. Bergmann, S. Kliesch, W. Weidner, K. Steger. Presence of histone H3 acetylated at lysine 9 in male germ cells and its distribution pattern in the genome of human spermatozoa. *Reprod. Fertil. Dev.* **2011**, *23*, 997.
- [13] J. Hardouin. Protein sequence information by matrix-assisted laser desorption/ionization in-source decay mass spectrometry. *Mass Spectrom. Rev.* **2007**, *23*, 672.
- [14] S. Nicolardi, L. Switzar, A. M. Deelder, M. Palmblad, Y. E. van der Burgt. Top-down MALDI-in-source decay-FTICR mass spectrometry of isotopically resolved proteins. *Anal. Chem.* **2015**, *87*, 3429.
- [15] F. G. Hanisch. Top-down sequencing of O-glycoproteins by in-source decay matrix-assisted laser desorption ionization mass spectrometry for glycosylation site analysis. *Anal. Chem.* **2011**, *83*, 4829.
- [16] D. Shechter, H. L. Dormann, D. C. Allis, S. B. Hake. Extraction, purification and analysis of histones. *Nat. Protocols* **2007**, *2*, 1445.
- [17] K. Maehara, A. Harada, Y. Sato, M. Matsumoto, K. I. Nakayama, H. Kimura, Y. Ohkawa. Tissue-specific expression of histone H3 variants diversified after species separation. *Epigenetics Chromatin* **2015**, *8*, 1.

- [18] D. Asakawa. Principles of hydrogen radical mediated peptide/protein fragmentation during matrix-assisted laser desorption/ionization mass spectrometry. *Mass Spectrom. Rev.* **2014**, *35*, 535.
- [19] R. Théberge, S. Dikler, C. Heckendorf, D. H. Chui, C. E. Costello, M. E. McComb. MALDI-ISD mass spectrometry analysis of hemoglobin variants: a top-down approach to the characterization of hemoglobinopathies. *J. Am. Soc. Mass Spectrom.* **2015**, *26*, 1299.
- [20] X. Su, C. Ren, M. A. Freitas. Mass spectrometry-based strategies for characterization of histones and their post-translational modifications. *Expert. Rev. Proteomics* **2007**, *4*, 211.

SUPPORTING INFORMATION

Additional supporting information may be found in the online version of this article at the publisher's website.